

Electronic Supplementary Information

RGD-functionalized ultrasmall iron oxide nanoparticles for targeted T₁-weighted MR imaging of glioma

Yu Luo,^{1a} Jia Yang,^{1b} Yu Yan,^a Jingchao Li,^a Mingwu Shen,^{*a} Guixiang Zhang,^{*b} Serge Mignani^c and Xiangyang Shi^{*a}

^a College of Chemistry, Chemical Engineering and Biotechnology, Donghua University, Shanghai 201620, People's Republic of China

^b Department of Radiology, Shanghai General Hospital, School of Medicine, Shanghai Jiaotong University, Shanghai 200080, People's Republic of China

^c Université Paris Descartes, PRES Sorbonne Paris Cité, CNRS UMR 860, Laboratoire de Chimie et de Biochimie pharmacologiques et toxicologique, 45, rue des Saints Pères, 75006 Paris, France

*To whom correspondence should be addressed. E-mail: xshi@dhu.edu.cn (X. Shi), guixiangzhang@sina.com (G. Zhang), mwshen@dhu.edu.cn (M. Shen),

¹ Authors contributed equally to this work.

Table S1. Zeta-potential and hydrodynamic size of the Fe₃O₄, Fe₃O₄-*m*PEG, and Fe₃O₄-PEG-RGD NPs.

Sample	Zeta potential (mV)	Hydrodynamic size (nm)
Fe ₃ O ₄	-39.7 ± 2.7	14.6 ± 1.2
Fe ₃ O ₄ - <i>m</i> PEG	-8.8 ± 0.6	168.7 ± 3.4
Fe ₃ O ₄ -PEG-RGD	-10.1 ± 0.4	212.5 ± 4.7

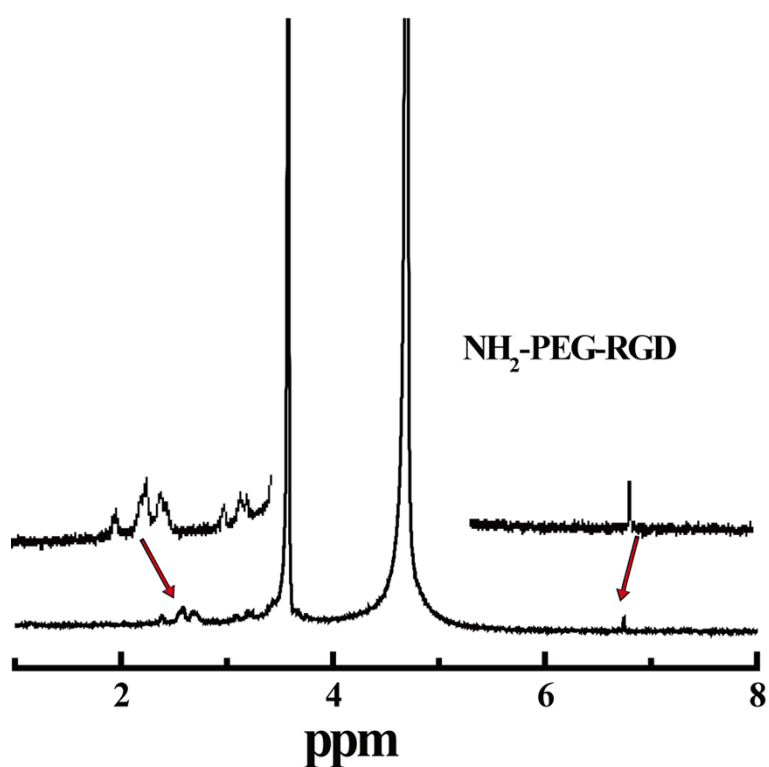


Figure S1. ¹H NMR of NH₂-PEG-RGD dissolved in D₂O.

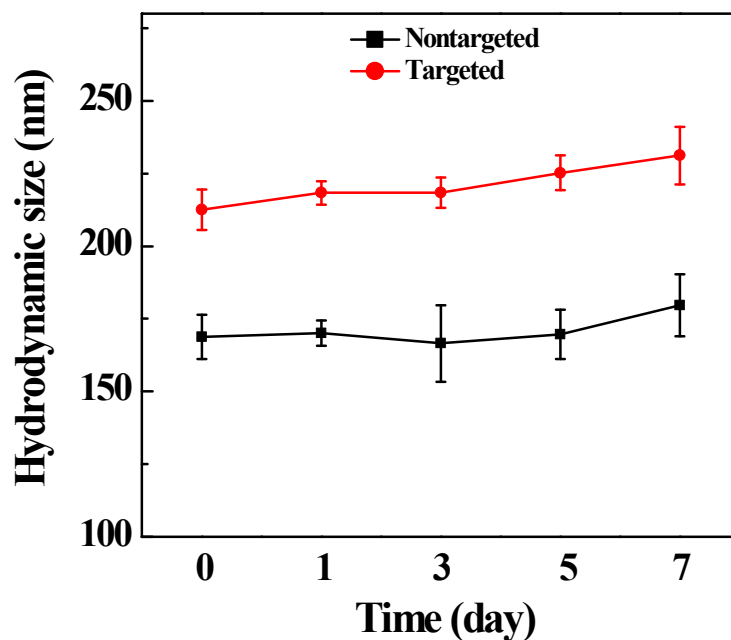


Figure S2. Hydrodynamic size of the Fe_3O_4 -*m*PEG (Nontargeted) and Fe_3O_4 -PEG-RGD (Targeted) NPs (1 mg/mL, dispersed in water) at different time periods.

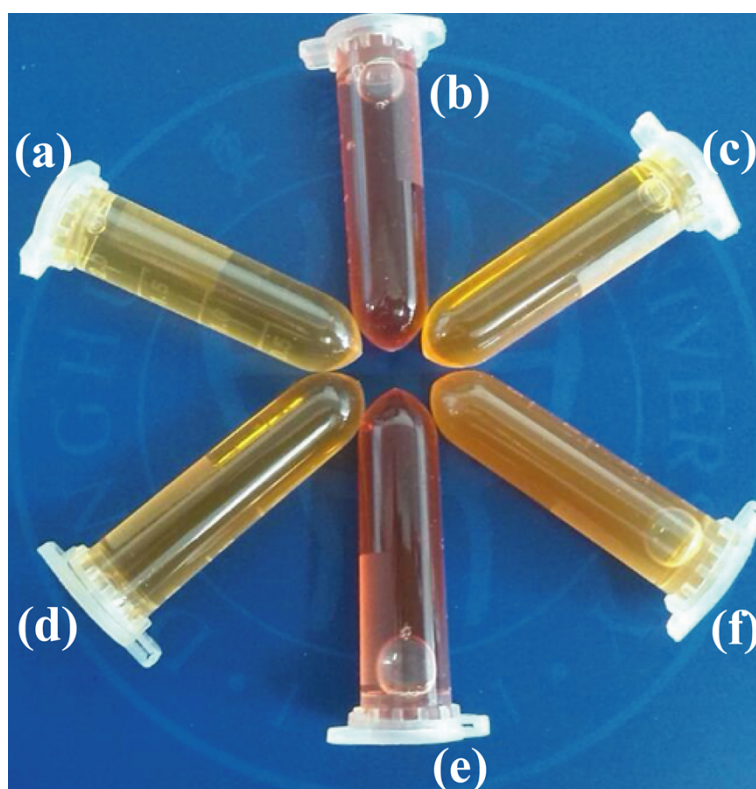


Figure S3. Photographs of the Fe_3O_4 -*m*PEG (a, b, c) and Fe_3O_4 -PEG-RGD (d, e, f) NPs dispersed in water (a, d), cell culture medium (b, e), and PBS (c, f) for two weeks.

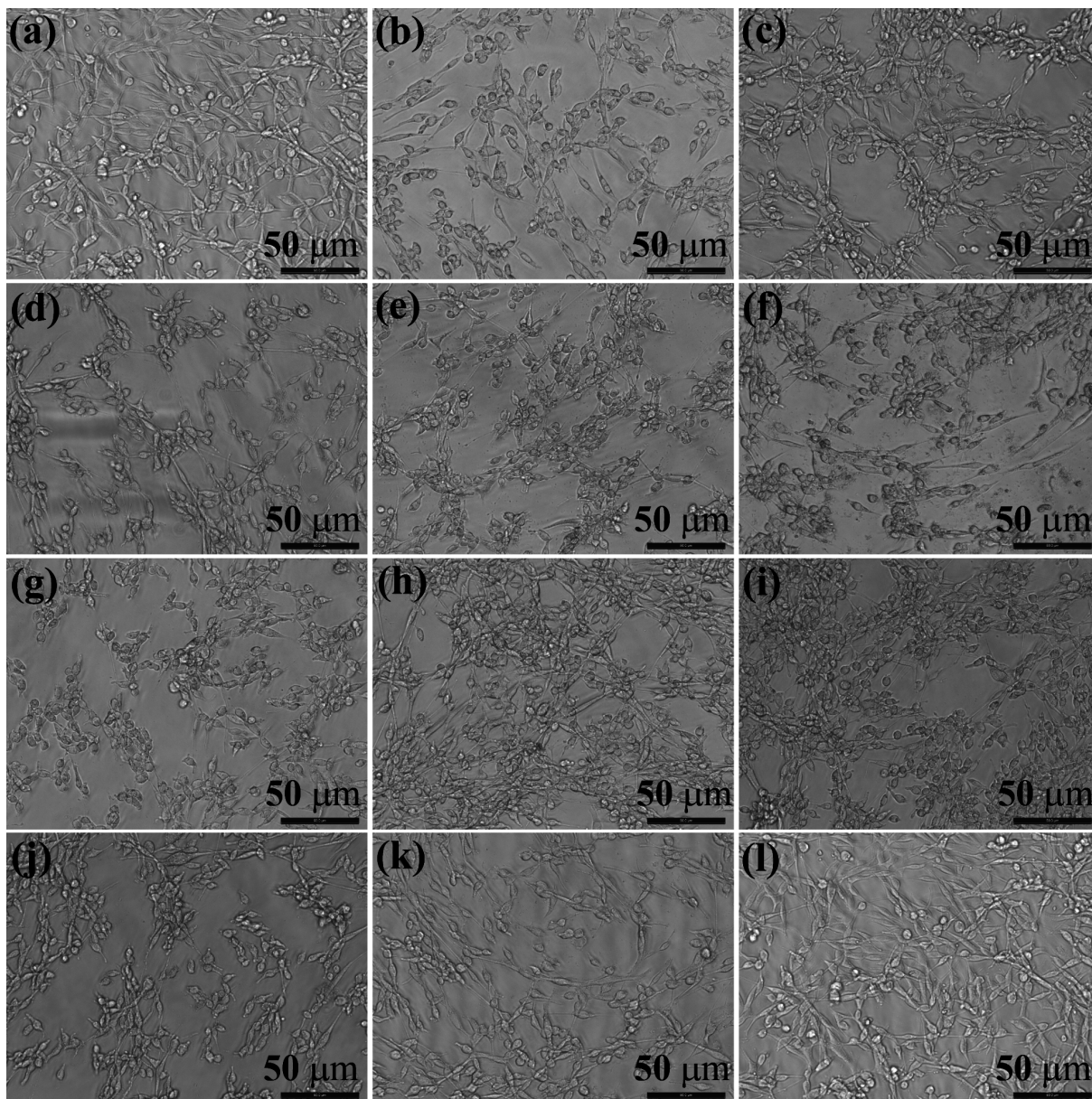


Figure S4. Photo micrographs of U87MG cells treated with PBS (a, l), the Fe_3O_4 -*m*PEG NPs at the Fe concentrations of 5 (b), 10 (c), 25 (d), 50 (e), and 100 (f) $\mu\text{g}/\text{mL}$, and the Fe_3O_4 -PEG-RGD NPs at the Fe concentrations of 5 (g), 10 (h), 25 (i), 50 (j), and 100 (k) $\mu\text{g}/\text{mL}$ for 24 h.

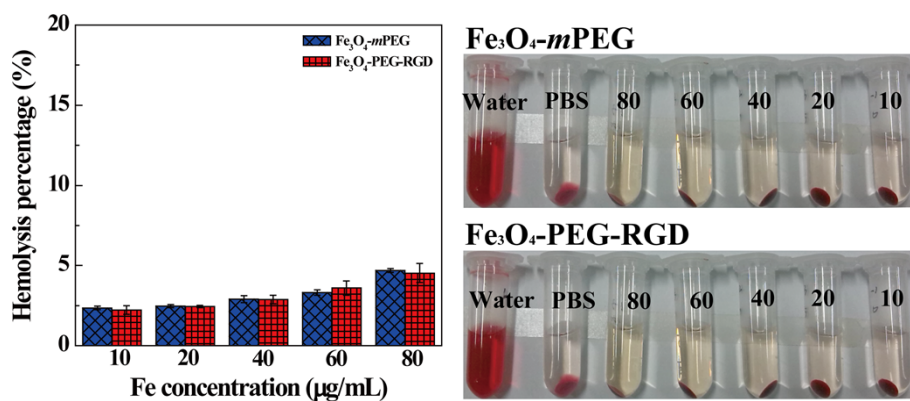


Figure S5. Hemolysis percentage (left panel) and photograph (right panel) of the HRBCs treated with the Fe_3O_4 -*m*PEG and Fe_3O_4 -PEG-RGD NPs with different Fe concentrations. The data are

expressed as mean \pm SD ($n = 3$). Water and PBS were used positive and negative control, respectively.

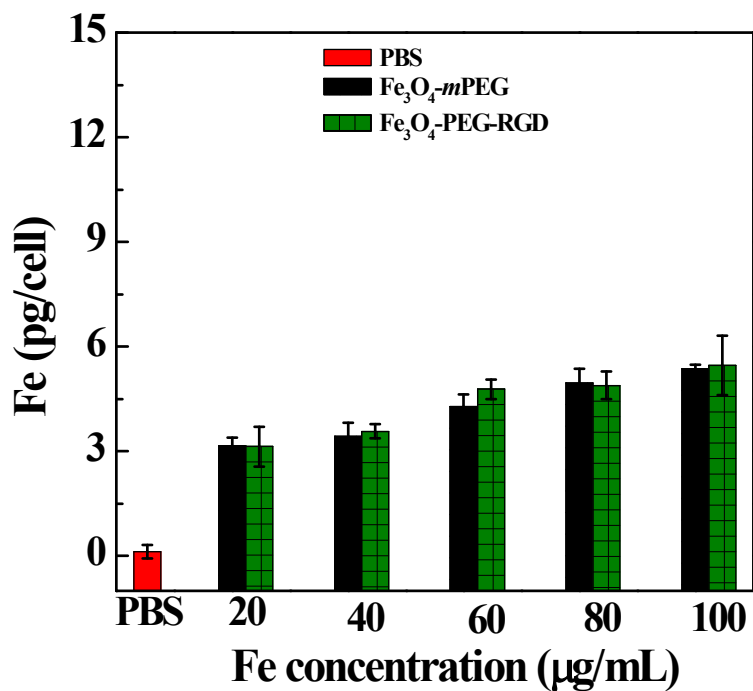


Figure S6. The Fe uptake in L929 cells after the cells were treated with the $\text{Fe}_3\text{O}_4\text{-mPEG}$ or $\text{Fe}_3\text{O}_4\text{-PEG-RGD}$ NPs with different Fe concentrations for 4 h. L929 cells treated with PBS were used as control.

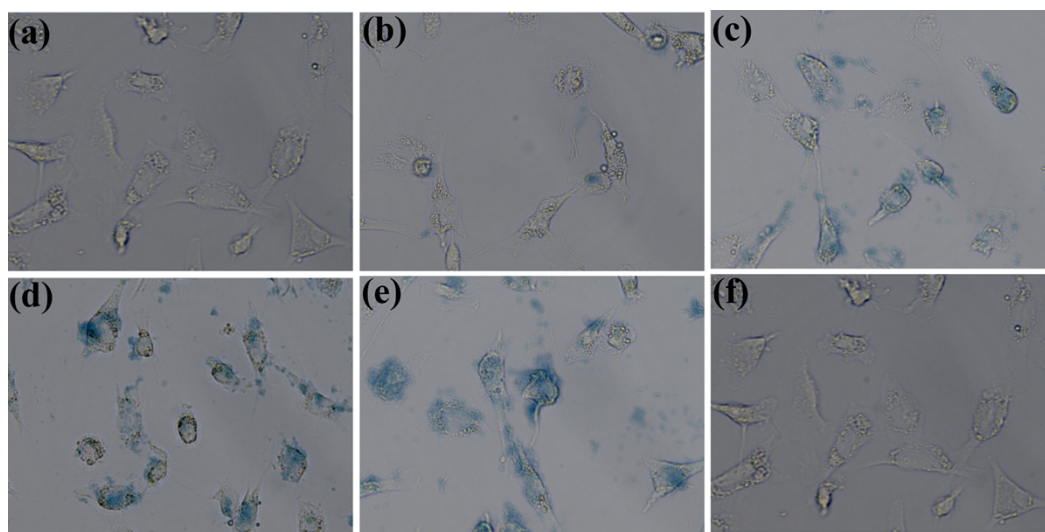


Figure S7. Prussian blue staining of U87MG cells after treated with the $\text{Fe}_3\text{O}_4\text{-mPEG}$ at the Fe concentration of 50 (b) and 100 (c) $\mu\text{g/mL}$ or $\text{Fe}_3\text{O}_4\text{-PEG-RGD}$ NPs at the Fe concentration of 50 (d), 100 (e) $\mu\text{g/mL}$, respectively for 4 h. U87MG cells treated with PBS were used as control (a and f).